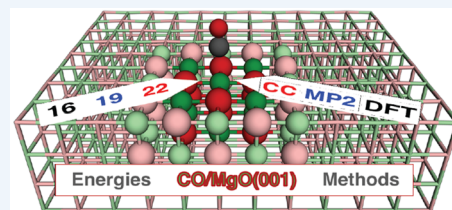


Ab Initio Calculations for Molecule–Surface Interactions with Chemical Accuracy

Joachim Sauer*¹

Institute of Chemistry, Humboldt University, 10117 Berlin, Germany

CONSPECTUS: Atomistic understanding of complex surface phenomena such as heterogeneous catalysis or storage and separation of energy-relevant gases in nanoporous materials (zeolites; metal–organic frameworks, MOFs) requires knowledge about reaction energies and energy barriers for elementary steps. This is difficult to obtain from experiment since the number of possible chemical, adsorption/desorption, and diffusion steps coupled to complex reaction networks is large, and so is the number of possible surface sites. Here is an important role of quantum chemistry which can provide rate and equilibrium constants for elementary steps “ab initio.” To be useful, the predictions have to reach chemical accuracy (4 kJ/mol) which is difficult to achieve because realistic models of the surface systems may comprise of the order of a thousand atoms. While density functional theory (DFT) as a rule cannot be trusted to yield results within chemical accuracy limits, methods that are accurate enough (Coupled Cluster with Single, Double, and perturbative Triple Substitution, CCSD(T)) cannot be applied because of their exponential scaling with system size.



This Account presents a hybrid high-level–low-level quantum method that combines DFT with dispersion for the full periodic system with second order Møller–Plesset perturbation theory (MP2) for the reaction site within a mechanical embedding scheme. In addition, to check if MP2 is accurate enough, we calculate Coupled Cluster (CC) corrections with Single, Double, and perturbatively treated Triple substitutions (CCSD(T)) for sufficiently small models of the reaction site. This multilevel hybrid MP2:DFT-D+ Δ CC method is shown to yield chemical accuracy for a set of 12 molecule–surface interaction systems for which reliable experimental data are available. For CO/MgO(001), the history of the experiment–theory comparison illustrates two problems: (i) Do experiment and theory look at the same surface site? (ii) Does theory calculate the same quantity as derived from experiment?

The hybrid MP2:DFT-D+ Δ CC data set generated includes the MgO(001) surface, the Mg₂(dobdc) metal–organic framework, and the proton forms of the CHA and MFI zeolites interacting with the H₂, N₂, CO, CO₂, CH₄, and C₂H₆ molecules. It serves two purposes. First, it will be useful for testing density functionals with respect to their performance for molecule–surface interactions. Second, it establishes the hybrid MP2:DFT-D+ Δ CC method as a reliable and powerful tool for ab initio predictions of adsorption and reaction energies as well as energy barriers when testing reaction mechanisms. For adsorption of small molecules in MOFs, isotherm predictions have reached a level of accuracy that deviations between theoretical predictions and experiments indicate sample imperfections. For elementary steps of the industrially important methanol-to-olefin process, our hybrid MP2:PBE+D+ Δ CC calculations yield rate constants in agreement with experiment within chemical accuracy limits, finally achieving for molecule–surface reactions which was possible so hitherto only for gas phase reactions involving not more than 10 atoms.

INTRODUCTION

The general theory of quantum mechanics is now almost complete... the difficulty is only that the exact application of these laws leads to equations that are much too complicated to be soluble. It therefore becomes desirable that approximate methods of applying quantum mechanics should be developed, which can lead to an explanation of the main features of complex atomic systems without too much computation. (Paul Dirac)¹

Atomistic understanding of complex surface phenomena such as heterogeneous catalysis or storage and separation of energy-relevant gases in nanoporous materials (metal–organic frameworks – MOFs, zeolites) requires knowledge of reaction energies and energy barriers for elementary steps. This is difficult to obtain from experiment alone since many chemical transformation, adsorption/desorption, and diffusion steps are

coupled into complex reaction networks, and there is usually a distribution of different active sites. Here is an important role of quantum chemistry which can provide rate and equilibrium constants for critical elementary steps “ab initio.” To be useful, the predictions have to be “chemically accurate” (error of about 1 kcal/mol to 4 kJ/mol) which is difficult to achieve because realistic models of the surface systems may comprise of the order of a thousand atoms.

While, as a rule, density functional theory (DFT) cannot be trusted to make predictions within chemical accuracy limits,^{2–4} methods that are accurate enough (Coupled Cluster with Single and Double and Perturbative Triple Substitution, CCSD(T))^{5,6} cannot be applied because of their exponential

Received: September 26, 2019

Published: November 25, 2019

scaling with the system size.⁷ Despite the fantastic progress made over the last decades in numerical quantum chemistry, the development of “approximate methods of applying quantum mechanics” to “complex atomic systems without too much computation”¹ has remained a challenge since the early days of quantum mechanics.

To cope with the huge computational problem of quantum mechanical (QM) calculations for large chemical systems, we apply a divide and conquer strategy that departs from two observations: (i) The highest QM level is not for all points of a potential energy surface (PES) required and (ii) the highest QM level is not for the whole system required.

Our hybrid high-level QM–low-level QM method combines DFT with dispersion⁸ for the full periodic system with second order Møller–Plesset perturbation theory (MP2) for the reaction site.^{9–13} We use a mechanical embedding scheme^{14–16} for structure optimization at the QM:QM level, and we calculate the difference between CCSD(T) and MP2 as single point energies at minima and saddle points of the PES for sufficiently small models of the reaction site.¹⁰ This defines a multilevel (hybrid MP2:DFT-D+ΔCC) method in the spirit of Pople’s “model chemistry”, for example, his G2 or G3 methods,¹⁷ but with the “model size” as another dimension in addition to the “electronic structure method,” “basis set,” and “structure optimization dimensions”. Figure 1 shows the hierarchy of models that has been adopted for the methylation of propene in the cavity of the zeolite H-MFI.¹⁸

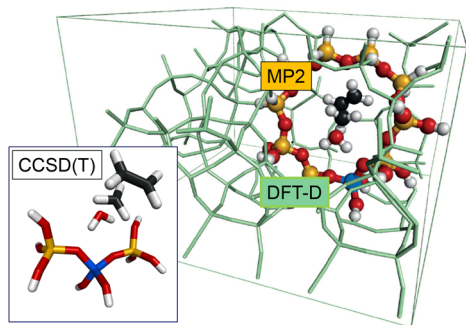


Figure 1. Hierarchy of models and methods for hybrid MP2:DFT-D + ΔCC calculations for the methylation of ethene on the Brønsted site of zeolite H-MFI. Adapted with permission from ref 20. Copyright 2016 John Wiley and Sons. The unit cell of the periodic structure is used for DFT calculations, whereas the colored ball-and-stick part shows the cluster model for MP2 calculations. The inset shows the model adopted for single point CCSD(T) calculations.

Our hybrid high-level cluster:low-level periodic approach shares with Morokuma’s Integrated MO:MO (IMOMO) approach which later became ONIOM,¹⁹ the mechanical embedding (“subtractive”) scheme for calculating energies and forces of a smaller cluster embedded in a larger system,¹⁶ but goes beyond ONIOM as periodic boundary conditions can be applied at the low level.^{14,15}

With mechanical embedding, the high-level wave function “feels” the environment only via changes of the structure, whereas the electronic interactions between the two regions are described at the low level only. Electronic embedding schemes face the problem of nonadditivity of the kinetic energy,²¹ but approximations have been proposed and efficient tools have been developed that can be applied to large chemical systems.^{22–24} Without structure optimization at the

hybrid level, subtractive schemes have been previously used to add high-level corrections for cluster models to low-level periodic calculations, e.g., for adsorption of small molecules on the MgO(001)²⁵ and TiO₂(110) surfaces.²⁶

■ HYBRID HIGH-LEVEL QM: LOW LEVEL QM METHODS

The hybrid MP2:DFT-D energy is defined by the subtractive scheme:

$$\begin{aligned} E_{\text{HL:LL}}(\text{pbc}, C) &= E_{\text{LL}}(\text{pbc}) - E_{\text{LL}}(C) + E_{\text{HL}}(C) \\ &= E_{\text{HL}}(C) + \Delta_{\text{LR}}(\text{pbc}, C) = E_{\text{LL}}(\text{pbc}) + \Delta_{\text{HL}}(C) \end{aligned} \quad (1)$$

The low-level (LL) energy of the surface model, $E_{\text{LL}}(\text{pbc})$, is obtained by a DFT calculation with periodic boundary conditions (pbc) and the high-level (HL) energy of the cluster, $E_{\text{HL}}(C)$, by a molecular calculation. The low-level energy of the cluster, $E_{\text{LL}}(C)$, is obtained by applying the same low-level method as used for the surface model. Thus, the long-range correction, $\Delta_{\text{LR}}(\text{pbc}, C)$, in eq 1 is evaluated at the low level, whereas the high-level correction, $\Delta_{\text{HL}}(C)$, is evaluated for the cluster.

Structure optimizations are also performed on the hybrid MP2:DFT-D potential energy surface using forces f defined according to^{14,15}

$$f_{\text{HL:LL}}(\text{pbc}) = f_{\text{LL}}(\text{pbc}) - f_{\text{LL}}(C) + f_{\text{HL}}(C) \quad (2)$$

We employ the MonaLisa code¹³ which allows to make use of energies and forces that are extrapolated to the complete basis set (CBS) limit^{27–29} and counterpoise corrected (CPC) for the basis set superposition error (BSSE).³⁰

To minimize boundary effects, we terminate the high-level (MP2) cluster models for zeolites and MOFs with hydrogen atoms.³¹ For ionic crystals like MgO, we found that embedding in point charges and full-ion effective core potentials does not have advantages compared to properly designed models without such embedding, in particular not when large polarized basis sets are used.¹² We refer to the original publications for details and stress that the right choice can be explored based on the magnitude of the long-range correction, $\Delta_{\text{LR}}(\text{pbc}, C)$. This requires calculations at the low, DFT-D, level only, for the periodic system which one needs anyway, and for the cluster model which is very fast.

The MP2 calculations on cluster models cure two deficiencies of DFT calculations:^{32,33}

(i) Insufficient description of dispersion. Among the different possibilities to account for dispersion in DFT (we will write DFT-D in the following),⁸ we prefer the simplest one - augmentation of existing exchange-correlation functionals with semiempirical atom-pair $1/r^6$ terms as customized by Grimme (D2 parametrization).³⁴ We have implemented an Ewald-like summation of the $1/r^6$ terms,³² thus avoiding cutoff parameters, and have shown that the atomic parameters derived for alkaline and alkaline-earth atoms are not applicable to the respective cations in ionic crystals. For Mg^{2+} , we found that the Mg parameters derived for atoms should be replaced by those of the isoelectronic noble gas atom (Ne).¹¹

(ii) Self-interaction correction (SIC) error. With periodic boundary conditions (pbc) almost exclusively functionals of GGA-type (Generalized Gradient Approximation) are applied which—due to SIC errors - typically overstabilize polar structures such as carbenium ions in zeolites³³ and predict to

Table 1. Molecule–surface Interactions for Which Agreement between Experiment and ab Initio Calculations Has Been Achieved within Chemical Accuracy Limits^a

system	ΔE	ΔE	ΔE_{ref}	$\Delta E - \Delta E_{\text{ref}}$	ΔH
	PBE+D2	hybrid	expt ref	dev	expt
CO/MgO(001)	-22.1	-21.2 ± 0.5 ³⁷	-20.6 ± 2.4 ¹²	-0.6 ± 2.9	-16.5 ⁴⁴
CH ₄ /MgO(001)	-14.8	-14.0 ± 1.0 ¹³	-15.0 ± 0.6	1.0 ± 1.6	-12.2 ⁴⁵
C ₂ H ₆ /MgO(001)	-23.9	-23.3 ± 0.6 ¹³	-24.4 ± 0.6	1.1 ± 1.2	-22.1 ⁴⁵
H ₂ /MOF-5	-9.6	-8.0 ± 0.4 ³⁸	-8.1 ± 0.8	0.1 ± 1.2	-6.6, ⁴⁶ -6.3 ± 0.5 ⁴⁷
CO/CPO-27-Mg ^b	-41.5	-43.3 ± 1.4 ³⁹	-43.8 ± 1.0	0.5 ± 2.4	-39.8 ± 1.0 ⁴⁸
CO ₂ /CPO-27-Mg ^b	-41.5	-48.8 ⁴⁰	-46.2	-2.6	-43.5 ⁴⁹
CH ₄ /H-CHA	-34.7	-25.3 ⁴¹	-27.2	1.9	-17.0
C ₂ H ₆ /H-CHA	-45.8	-36.2 ⁴¹	-33.5	2.7	-27.5
C ₃ H ₈ /H-CHA	-57.3	-46.7 ⁴¹	-43.8	2.9	-37.6
		ΔE^{\ddagger}	$\Delta E_{\text{ref}}^{\ddagger}$	$\Delta E^{\ddagger} - \Delta E_{\text{ref}}^{\ddagger}$	ΔH^{\ddagger}
barriers	PBE+D2	hybrid	expt ref	dev	expt
C ₂ H ₄ /CH ₃ OH-H-MFI	79.2	93.6 ²⁰	93.4	-0.2	104 ⁵⁰
C ₃ H ₆ /CH ₃ OH-H-MFI	32.7	51.9 ²⁰	53.4	1.5	64 ⁵¹
C ₄ H ₈ /CH ₃ OH-H-MFI	17.6	32.5 ²⁰	29.4	-3.1	40 ⁵¹

^aPBE+D2 and hybrid MP2:PBE+D2+ Δ CC energies and energy barriers, ΔE and ΔE^{\ddagger} , respectively, reference energies derived from experimental enthalpies (see eq 7), ΔE_{ref} and $\Delta E_{\text{ref}}^{\ddagger}$, as well as experimental enthalpies, ΔH_{T} and $\Delta H_{\text{T}}^{\ddagger}$, all in kJ/mol. ^bMetal–organic framework with Mg₂(dobdc) composition, dobdc⁴⁻ = 2,5-dioxido-1,4-benzenedicarboxylate, also known as Mg-MOF-74, loading 1:1: one molecule on each Mg²⁺ ion.

low energy barriers.³ For example, for the methylation of alkenes in zeolite H-MFI, after accounting for dispersion, we obtained systematically too low energy barriers.^{18,20} Because the SIC error is rather localized at the reaction site and converges quickly with the cluster size,^{32,33} the size of the MP2 cluster model in hybrid MP2:DFT-D calculations can be rather limited, see ref.³⁵ for a recent example.

For the hybrid MP2:DFT-D structure optimization, typically complete basis set (CBS) extrapolation with augmented triple- ζ and double- ζ basis sets would be used, CBS(D,T). To examine the effect of basis set extension, Δ_{basis} , single-point CBS(T,Q) or CBS(Q,5) calculations with quadruple (Q) or quintuple (5) basis sets may be performed, e.g.,

$$\Delta_{\text{basis}} = E_{\text{MP2}}[\text{CBS}(Q, 5)] - E_{\text{MP2}}[\text{CBS}(D, T)] \quad (3)$$

To examine the effect of convergence with the cluster size, $\Delta_{\text{LR}}(\text{pbc}, C) = E_{\text{LL}}(\text{pbc}) - E_{\text{LL}}(C)$ is evaluated for a second, larger cluster C^{large}. If the hybrid scheme worked perfectly, $E_{\text{HL,LL}}$ should not be affected and any change in $E_{\text{DFT-D}}(C)$ should be compensated by the corresponding change in E_{MP2} , i.e., the ratio

$$F = \frac{E_{\text{MP2}}(C^{\text{large}}) - E_{\text{MP2}}(C_{\text{opt}})}{E_{\text{DFT-D}}(C^{\text{large}}) - E_{\text{DFT-D}}(C_{\text{opt}})} \quad (4)$$

should be 1. In practice, it is not, but as suggested previously³⁶ the ratio F can be used to improve $E_{\text{MP2:DFT-D}}$ by scaling Δ_{LR} .

$$E_{\text{MP2}}(\text{pbc}) \approx E_{\text{MP2:DFT-D}}(\text{pbc}, C_{\text{opt}}) + \Delta_{\text{basis}} + F \cdot \Delta_{\text{LR}}(C_{\text{large}}) \quad (5)$$

As a final step, at the hybrid MP2:DFT-D equilibrium structures, CCSD(T) “single point” calculations are carried out for smaller cluster models, C_{CC}. CCSD(T) correlation effects are estimated as $\Delta_{\text{CCSD(T)}} = E_{\text{CCSD(T)}} - E_{\text{MP2}}$ differences, and the final estimate of the CCSD(T) energy for the periodic system becomes

$$E_{\text{CCSD(T)}}(\text{pbc}) \approx E_{\text{MP2}}(\text{pbc}) + \Delta_{\text{CCSD(T)}}(C_{\text{CC}}) \quad (6)$$

Our standard computational protocol involves the following steps:³⁷

- (1) DFT-D calculations
 - (1a) structure optimization
 - (1b) harmonic force constants for characterizing stationary points and vibrational energies
 - (1c) zero-point vibrational energies, thermal enthalpy contributions
- (2) hybrid MP2:DFT-D structure optimizations
- (3) single point calculations at the hybrid MP2:DFT-D structure
 - (3a) MP2 cluster calculations with larger basis sets for than used in optimization
 - (3b) second (larger) cluster size for scaling Δ_{LR}
- (4) CCSD(T) single point calculations for a smaller cluster

Sometimes, the MP2:DFT-D structure optimization (step2) can be skipped and all calculations are performed as single-point calculations at the DFT-D structure.

SYSTEMS WITH CHEMICALLY ACCURATE MOLECULE–SURFACE INTERACTION ENERGIES

Our hybrid MP2:DFT-D+ Δ CC method has been applied to a set of 12 molecule–surface interactions for which experimental data were available:

- (i) adsorption of CO,^{12,37} as well as CH₄ and C₂H₆ on the MgO(001) surface¹³
- (ii) adsorption of H₂ in MOF-5,³⁸ and of CO³⁹ and CO₂⁴⁰ in MOF Mg₂(dobdc) with dobdc⁴⁻ = 2,5-dioxido-benzenedicarboxylate
- (iii) adsorption of CH₄, C₂H₆, and C₃H₈ in zeolite H-chabazite⁴¹
- (iv) energy barriers for methylation reactions of small alkenes in zeolite H-MFI²⁰

In the absence of periodic boundary CCSD(T) results for molecule–surface interactions, comparison with experiments is

the way to judge the performance of our hybrid MP2:DFT-D+ Δ CC method. Making this comparison, first, we need to be aware of the accuracy limits of CCSD(T) itself, for which ± 2 kJ/mol may be a fair judgment.^{42,43}

Further, we need to make sure that we do not compare apples and oranges. Whereas QM calculations report energies of adsorption (bottom of the potential energy well), ΔE , experiments usually yield enthalpies of adsorption, ΔH_T , that depend on temperature, T . For comparison with QM energies we need to convert the enthalpies into “experimentally derived” reference energies, ΔE_{ref} , taking zero-point vibrational energies, ΔE_{ZPV} , and thermal enthalpy changes, $\Delta_T \Delta H$, into account.^{12,41}

$$\Delta E_{\text{ref}} = \Delta H_T(\text{exp}) - \Delta_T \Delta H(\text{DFT} - \text{D}) - \Delta E_{\text{ZPV}}(\text{DFT} - \text{D}) \quad (7)$$

The latter we calculate from vibrational partition functions using our low-level method (DFT-D) which adds some uncertainty (of the order of 0.5 kJ/mol) to the uncertainty of the experimental values.

Table 1 shows that for all 12 systems, agreement between QM calculations and experiment has been reached within chemical accuracy limits. For the reaction of ethene, propene, and 1-butene with methanol in zeolite H-MFI, kinetic experiments have been performed in such a way that reliable reaction rates and activation energies for single reaction steps could be obtained and serve as benchmark for quantum chemical calculations.¹⁸ For these reactions, hybrid MP2:PBE+D2+ Δ CC calculations (see Figure 1 for the models used) not only yielded enthalpy barriers in agreement with experiment within chemical accuracy limits (Table 1), but also the predicted pre-exponentials (activation entropies) and rate constants showed agreement with experiment within 1 order of magnitude.²⁰ This was only possible because anharmonicity was included in the vibrational partition functions within transition state theory.

The data set in Table 1 serves two purposes:

First, it demonstrates that the hybrid MP2:DFT-D+ Δ CC method is a reliable and powerful tool for *ab initio* predictions of adsorption and reaction energies as well as energy barriers when testing reaction mechanisms, see refs.^{33,35,52} A few examples will be presented below.

Second, it will be useful for testing density functionals (and other approximate QM methods or force fields) with respect to their performance for molecule–surface interactions, and as such will constitute a significant extension of test sets available in the literature for many other types of chemical interactions. Our test results for different ways of including dispersion in DFT will be published elsewhere. The PBE+D2 results in Table 1 have been obtained as low-level part of our hybrid approach. Their deviation from the hybrid results varies widely, from less than 4 kJ/mol (chemical accuracy) to as much as 10 kJ/mol for hydrocarbon adsorption or up to 20 kJ/mol for energy barriers.

■ CO ON MgO(001): THE HYDROGEN MOLECULE OF SURFACE SCIENCE

Quantum mechanics was not considered right before agreement between experiment (Herzberg) and theory (Kolos and Wolniewicz) had been reached for the dissociation energy of the H₂ molecule.⁵³ A quantum mechanical method will not get molecule–surface interactions right if it does not get CO

adsorption on the MgO(001) surface right. The story of attempts to meet this challenge has been told by Pacchioni⁵⁴ until the year 2000 (see also ref 55), and it is continued here into the new millennium; see Figure 2.

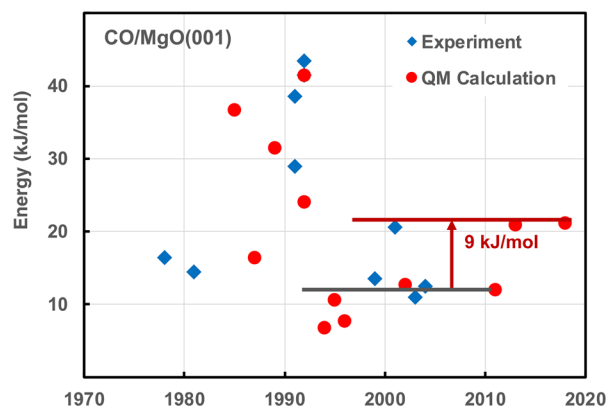


Figure 2. Binding energies (kJ/mol) of CO on the MgO(001) surface: experiment and theory over the years. Data from ref 55, augmented with data mentioned in the text.

There are two questions: Do experiment and theory yield the same physical quantity? (ΔH vs ΔE ; see above), and do experiment and theory look at the same surface site? In experiment, even if the sample exposes a defined crystallographic plane like MgO(001), defects and multilayer desorption may lead to peaks in the temperature-programmed desorption (TPD) plot, and it was not before the crucial study of Kühlenbeck, Freund and co-workers⁵⁶ that a desorption peak at 57 K was safely assigned to the five-coordinated terrace sites on the MgO(001) surface. The surface coverage also matters. Lateral interactions can be either repulsive, as the dipole–dipole interactions for CO/MgO(001), or attractive, as the dispersion interactions for CH₄/MgO(001). When cluster calculations are performed, they refer to isolated sites, i.e., a coverage approaching zero. In contrast, when periodic boundary conditions are applied, low coverages would require large unit cells, but to cope with the exponential increase in computer resources with system size, often small unit cells are chosen corresponding to unrealistically high loadings. In our study on CO/MgO(001),^{12,37} we occupy 1/8 of the Mg²⁺ terrace sites with CO and compare with an experimental value⁴⁴ for the same coverage.

When Pacchioni wrote his review on CO/MgO(001),⁵⁴ experiment⁵⁶ and calculations seemed to have converged to a value close to 10 kJ/mol for the adsorption energy;^{54,55} see Figure 2. Two years later, this was confirmed by the hybrid MP2:B3LYP calculations of Damin and Ugliengo who obtained 12.7 kJ/mol,²⁵ in apparently close agreement with experiment (13.5 kJ/mol).⁵⁶ Moreover, in 2004, the experimental result for the single crystal surface had seemingly been confirmed with high surface area powder samples.⁵⁷ A ΔH value of 12.5 ± 0.1 kJ/mol was obtained from a van't Hoff plot (Figure 22 in ref 57) assuming a linear relation between IR intensity and surface coverage and based on a Langmuir isotherm. The difference of 1.5 kJ/mol from a previous IR derived ΔH value (11 kJ/mol)⁵⁸ was ascribed to differences in the integration over the CO band shape which already hints to an uncertainty of at least 1.5 kJ/mol for ΔH values derived from temperature dependent IR spectra, but the uncertainty

may be much larger. For CO adsorbed in MOF Mg₂(dobdc) which shares with the MgO(001) surface the 5-fold coordinated Mg²⁺ sites, the IR derived ΔH value is 6 kJ/mol less binding than the value derived from the isotherm measurements.³⁹

With the hybrid MP2:DFT-D+ Δ CC method presented in this Account, we obtained a binding energy of 21.0 kJ/mol with an estimated uncertainty of ± 1 kJ/mol.¹² The apparent deviation from experiment was 7.5 kJ/mol, clearly outside the chemical accuracy range. We dared to submit the manuscript, and a helpful reviewer told us that we had overlooked another TPD study already published in 2001 which reported a desorption energy of 18.5 ± 2.0 kJ/mol.⁴⁴ Now the calculated energy agreed with the experimental reference energy (20.6 ± 2.4 kJ/mol, Table 2) within 0.4 ± 3.4 kJ/mol. Recently, we

Table 2. Derivation of “Experimental” Reference Desorption Energies from TPD Experiments (kJ/mol)

	expt	
	Wichtendahl et al. ⁵⁶	Dohnalek et al. ⁴⁴
pre-exponential, $\log \nu$ (s ⁻¹)	13	15 ± 2
E_d^A	13.5 ± 1.1^a	18.5 ± 2.0^b
T/K	57	60
$-RT - \Delta H(T)^c$	-1.9	-1.9
$-\Delta E_{zvp}^c$	4.0 ± 0.4^d	4.0 ± 0.4^d
E^d	16.5 ± 1.5	20.6 ± 2.4

^aUncertainty due to change of pre-exponential by 1 order of magnitude. ^bFor coverage $\theta = 1/8$. ^cHarmonic wavenumbers from PBE+D2 slab calculations. ^dFor uncertainty estimate, see ref 12, section 4.1.

repeated the hybrid MP2:DFT-D+ Δ CC calculations improving on both the hybrid MP2:DFT-D optimization and the CCSD(T) calculations.³⁷ The binding energy (21.2 ± 2.4 kJ/mol) changed by 0.2 kJ/mol only, which demonstrates the stability of our hybrid MP2:DFT-D+ Δ CC method with respect to reasonable choices of the details of the computational protocol.

Why were the two TPD results so different? As usual, ref 56 applied the Redhead equation to convert the desorption temperature into a desorption energy, which requires a guess of the pre-exponential. The common value of 10^{13} was chosen. In contrast, Dohnálek et al.⁴⁴ measured TPD curves for

different loadings. Fitting them based on the Polanyi–Wigner equation not only provided coverage dependent desorption energies but also yielded a value of $10^{15\pm 2}$ for the pre-exponential.

For both TPD experiments, Table 2 shows the conversion of experimental ΔH values in experimentally derived reference ΔE values according to eq 1. Moreover, TPD desorption energies are Arrhenius activation energies of desorption, E_A , which differ from the desorption enthalpy by RT (R is the gas constant)

$$\Delta H_T = E_A - RT \quad (8)$$

Table 2 shows that previous quantum chemical studies^{25,54} should have made comparison with the energy value of 16.5 kJ/mol rather than with the Arrhenius barrier of 13.5 kJ/mol reported by Wichtendahl et al.⁵⁶ However, the proper reference value derived from the TPD experiments of Dohnalek et al. is 20.6 ± 2.4 kJ/mol, 7 kJ/mol larger than the experimental value used as benchmark before. This difference is far outside the chemical accuracy range which underlines the importance of proper analysis of experimental results when assessing the accuracy of QM results.

■ ADSORPTION ISOTHERMS AND STRUCTURAL IMPERFECTIONS OF MOFs

With the hybrid MP2:DFT-D+ Δ CC method presented, the prediction of adsorption isotherms for MOFs has reached a level of accuracy that structural surface models can be tested; i.e., deviations between predicted isotherms for the ideal structure and measured isotherms may point to imperfections of the sample. For H₂ in MOF-5,³⁸ Figure 3 (left) shows deviations between measured isotherms that are clearly outside the estimated uncertainty range of the calculations (0.4 wt % at 40 bar).³⁸ That the measured pore volumes of samples synthesized in 1999 and 2005 increased from 1.05 to 1.56 cm³/g⁵⁹ also underlines the role of the sample quality. The lack of reproducibility of measured adsorption isotherms has become a major concern for the rational design of improved MOFs.⁶⁰

The CH₄/Mg₂(dobdc) adsorption isotherms (Figure 3, right) calculated for the ideal material overestimate the predicted excess amounts of adsorbed CH₄, which indicates that parts of the sample are not accessible for guest molecules. Indeed, measured isosteric heats of adsorption as function of

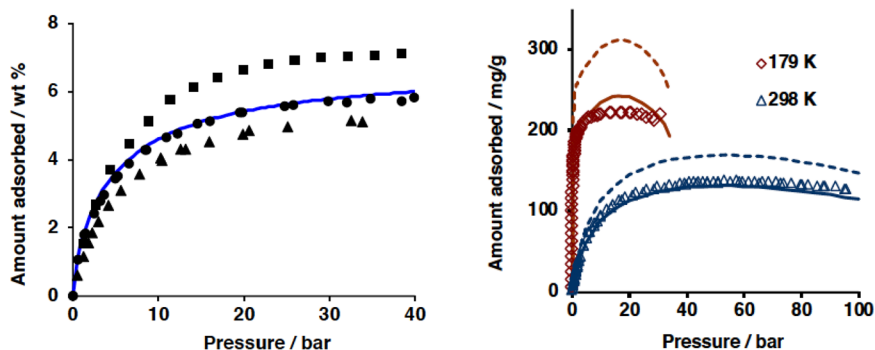


Figure 3. Adsorption isotherms. Hybrid QM:QM calculations for ideal crystalline structures compared to experiment. Left: H₂ in MOF-5. Adapted with permission from ref 38. Copyright 2009 American Chemical Society. Blue line, calculations for the ideal material; symbols (squares, dots, triangles), different experiments. Right: Excess adsorption isotherms for CH₄ in Mg₂(dobdc) at two different temperatures. Adapted with permission from ref 61. Copyright 2012 American Chemical Society. Dashed line, calculations for the ideal material; solid lines, calculations which assume experimentally determined availability (78%) of adsorption sites; symbols (diamonds and triangles), experiment.

loading suggest that only 78% of the sites in this crystal are available for adsorption, “because of a reduced rate of diffusion at such loadings or because the remaining metal sites are physically obstructed from access because of defects in the crystal structure.”⁶² Figure 3 shows that calculated isotherms assuming 78% available sites are in good agreement with measured isotherms.

REACTION MECHANISMS IN ZEOLITE CATALYSIS

Catalytic hydrocarbon conversion and synthesis by zeolites involve complex reaction networks with many chemical transformation adsorption/desorption and diffusion steps. Experimental information about individual elementary steps or short-lived intermediates is difficult to get from experiments which makes discrimination between different mechanistic proposals difficult if not impossible. Here is an important role of computational chemistry, but to be useful predictions have to be made with chemical accuracy.

Carbocations are often postulated as intermediates, but conclusive experimental evidence for the existence in zeolites of the smallest, possibly stable species, the *tert*-butyl cation could not be produced so far. Hybrid MP2:PBE+D2+ Δ CC calculations for zeolite H-FER confirmed that the *tert*-butyl cation is a (meta-)stable intermediate but showed that it is about 36 kJ/mol less stable than the isobutoxide and 50 kJ/mol less stable than the parent isobutene adsorbed at the Brønsted site (enthalpies at 298 K).^{10,33} Since the entropy loss is larger for the framework-bound alkoxide than for the mobile carbenium ion, the latter becomes relatively more stable with increasing temperature. In contrast, the difference between carbenium ion and adsorbed alkene does not change because they are equally mobile.⁶³ The barrier separating the *tert*-butyl cation from the adsorbed isobutene is 17.5 ± 5.0 kJ/mol. This translates into an estimated half-life time of 10–450 μ s for the *tert*-butyl cation once it is formed,³³ which is probably not long enough for detection by NMR.

For the alkylation of benzene with ethene on zeolite H-MFI hybrid MP2:PBE+D2+ Δ CC adsorption enthalpies and intrinsic enthalpy barriers have been calculated for both a one-step and a two-step mechanism. The conclusion has been reached that, under experimental conditions, the reaction proceeds in one-step and is apparent with respect to ethene and intrinsic with respect to benzene. The calculated apparent activation energy (66 kJ/mol) agrees with experiment (58–76 kJ/mol) within experimental uncertainty limits.

The consecutive methylations of small alkenes with methanol^{18,20,50,51} (see also Table 1) are crucial steps of the hydrocarbon pool mechanism for industrially relevant zeolite-catalyzed methanol-to-olefine (MTO) and methanol-to-hydrocarbon (MTH) processes which are of topical interest because C–C bonds are formed from C1 species. A single-point variant of hybrid MP2:PBE-D3 calculations has been recently used to calculate rate constants for 42 steps of the MTO initiation reactions and 63 steps of the autocatalytic alkene cycle for zeolite H-CHA.⁶⁴ A microkinetic model showed that first methanol is dehydrogenated to CO which subsequently reacts with methanol forming the first C–C bond. Our hybrid MP2:PBE+D2+ Δ CC method has been employed to make predictions for enthalpies and entropies of methanol (and ethanol) adsorption in H-MFI.⁶⁵

Proton exchange is the most elementary reaction step in alkane activation by zeolitic Brønsted sites. For methane in H-MFI and H-FER, apparent barriers between 108 and 117 kJ/

mol have been predicted by hybrid MP2:PBE+ Δ CC calculations in agreement with barriers derived from NMR-(H-MFI) and IR (H-FER) experiments.⁶⁶ In H-MFI, 50–60 kJ/mol lower barriers have been measured for *i*-butane than for *n*-butane, both using NMR⁶⁷ and batch reactor experiments; see Figure 4. This has triggered a debate whether proton

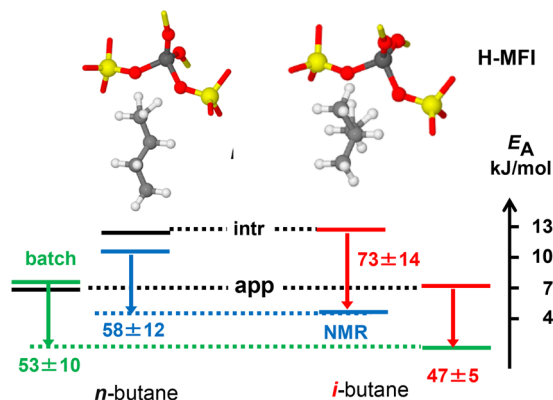


Figure 4. Intrinsic (intr) and apparent (app) enthalpy barriers compared to NMR experiments (NMR) and batch recirculation reactor experiments (batch), respectively, for *n*-butane and *i*-butane in zeolite H-MFI. Data from ref 35.

exchange occurs directly via carbonium type transition structures⁶⁷ or indirectly via hydride transfer between the alkane and a *tert*-butyl carbenium.^{68,69} To solve this mechanistic problem, hybrid MP2:PBE+D2+ Δ CC calculations of enthalpy barriers have been performed.³⁵ A change to the indirect proton exchange mechanism with *i*-butane could be excluded, because the barrier for dehydrogenation of *i*-butane that would create a *tert*-butyl cation is much too high, 188 and 132 kJ/mol for the intrinsic and apparent enthalpy barrier, respectively, at 500 K. The predicted intrinsic and apparent barriers for the direct proton exchange step are the same for *i*-butane as for *n*-butane within 2–5 kJ/mol. Given that the calculations are chemically accurate, this implies that the observed *i*-butane reactivity cannot be rationalized with the ideal zeolite structure featuring bridging hydroxyls as Brønsted acid sites as assumed in the calculations. This points to a possible involvement of other active sites with *i*-butane, for example, in connection with extraframework aluminum species. Indeed, Schoofs et al. observed for *i*-butane that “...in the absence of extra-lattice aluminum, the [proton] exchange rate is zero or very small.”⁶⁹ and Lercher and co-workers showed that the “activity [of H-MFI catalysts] passes through a maximum for zeolites having experienced short steaming durations” and explained this with formation of “transient partially framework-bound Al-species”.⁷⁰ We also note that the proton exchange experiments on *n*-butane and *i*-butane have not been made on the same sample and the conclusion has been reached “that further clarification needs experimental studies that compare *n*-butane and *i*-butane on the same set of H-MFI samples with as much as possible control and characterization of such species.”³⁵

CONCLUDING REMARKS

Up to now, the prediction of energy barriers and rate constants “with an accuracy comparable to (or even exceeding) experimental precision”⁷¹ was possible only for gas phase reactions involving not more than ten atoms. The hybrid

MP2:PBE+D2+ Δ CC predictions of energy barriers and rate constants for the methylation of alkenes in zeolites show that this goal has finally been reached also for molecule–surface reactions. In a highlight article, Richard Catlow states:⁷² “...Chemical accuracy has been achieved for real and significant catalytic processes. We now have procedures that will enable the calculation of reaction rates for heterogeneously catalyzed reactions within experimental error” and he concludes “...computational modelling has now reached the stage where it can provide reliable and quantitative rates of catalytic reactions, and this achievement is a very significant milestone in the field.”

The subtractive hybrid QM:QM scheme for molecule–surface interactions presented here has the advantage that it is perfectly scalable and immediately can take advantage of improved algorithms and implementations of MP2 or CCSD(T) codes. It is also general enough to envision its future extension to systems for which MP2 is no longer a good first approximation and/or CCSD(T) does not yield chemical accuracy. This includes cases that require a multireference treatment as high-level method or cases that involve metal surfaces for which RPA (random phase approximation)^{73,74} could be considered as high-level method.

AUTHOR INFORMATION

Corresponding Author

*E-mail: js@chemie.hu-berlin.de.

ORCID

Joachim Sauer: 0000-0001-6798-6212

Notes

The author declares no competing financial interest.

Biography

Joachim Sauer is Senior Researcher at Humboldt University in Berlin where he was Professor of Theoretical Chemistry from 1993–2017. He is external scientific member of the Fritz Haber Institute (Max Planck Society) and, until 2018, was a member of the cluster of excellence “Unifying Concepts in Catalysis”. His research has explored the application of quantum chemical methods in cluster chemistry, heterogeneous catalysis and adsorption in nanoporous materials, particularly for transition metal oxides, zeolites and metal–organic frameworks.

ACKNOWLEDGMENTS

I thank all the doctoral students and postdocs who did the work that is described in this Account and who are coauthors of the original publications cited, in particular Maristella Alessio, Arpan Kundu, Giovanni Piccini, Kaido Sillar, and Christian Tuma. This work has been supported by German Research Foundation, in particular by a Reinhart Koselleck-Grant and by a project grant within the priority program 1570 “Porous media with defined pore structure”, as well as by computer time grants from the North German Computing Alliance Berlin–Hannover (HLRN). I am grateful to the “Fonds der Chemischen Industrie” and the International Max Planck Research School “Functional Interfaces in Physics and Chemistry” at the Fritz Haber Institute of the Max Planck Society, Berlin for fellowships to doctoral students.

REFERENCES

- (1) Dirac, P. A. M. Quantum Mechanics of Many Electron Systems. *Proc. R. Soc. London, Ser. A* **1929**, *123*, 714–733.
- (2) Neese, F.; Hansen, A.; Wennmohs, F.; Grimme, S. Accurate Theoretical Chemistry with Coupled Pair Models. *Acc. Chem. Res.* **2009**, *42*, 641–648.
- (3) Zhao, Y.; Truhlar, D. G. Design of Density Functionals That Are Broadly Accurate for Thermochemistry, Thermochemical Kinetics, and Nonbonded Interactions. *J. Phys. Chem. A* **2005**, *109*, 5656–5667.
- (4) Mallikarjun Sharada, S.; Bligaard, T.; Luntz, A. C.; Kroes, G.-J.; Nørskov, J. K. SBH10: A Benchmark Database of Barrier Heights on Transition Metal Surfaces. *J. Phys. Chem. C* **2017**, *121*, 19807–19815.
- (5) Urban, M.; Noga, J.; Cole, S. J.; Bartlett, R. J. Towards a full CCSDT model for electron correlation. *J. Chem. Phys.* **1985**, *83*, 4041–4046.
- (6) Raghavachari, K.; Trucks, G. W.; Pople, J. A.; Head-Gordon, M. A fifth-order perturbation comparison of electron correlation theories. *Chem. Phys. Lett.* **1989**, *157*, 479–483.
- (7) Sparta, M.; Neese, F. Chemical applications carried out by local pair natural orbital based coupled-cluster methods. *Chem. Soc. Rev.* **2014**, *43*, 5032–5041.
- (8) Grimme, S.; Hansen, A.; Brandenburg, J. G.; Bannwarth, C. Dispersion-Corrected Mean-Field Electronic Structure Methods. *Chem. Rev.* **2016**, *116*, 5105–5154.
- (9) Tuma, C.; Sauer, J. A hybrid MP2/plane wave-DFT Scheme for Large Chemical Systems: Proton Jumps in Zeolites. *Chem. Phys. Lett.* **2004**, *387*, 388–394.
- (10) Tuma, C.; Sauer, J. Treating Dispersion Effects in Extended Systems by Hybrid MP2:DFT Calculations—Protonation of Isobutene in Zeolite Ferrierite. *Phys. Chem. Chem. Phys.* **2006**, *8*, 3955–3965.
- (11) Tosoni, S.; Sauer, J. Accurate Quantum Chemical Energies for the Interaction of Hydrocarbons with Oxide Surfaces: CH₄/MgO(001). *Phys. Chem. Chem. Phys.* **2010**, *12*, 14330–14340.
- (12) Boese, A. D.; Sauer, J. Accurate Adsorption Energies of Small Molecules on Oxide Surfaces: CO-MgO(001). *Phys. Chem. Chem. Phys.* **2013**, *15*, 16481–16493.
- (13) Alessio, M.; Bischoff, F. A.; Sauer, J. Chemically accurate adsorption energies for methane and ethane monolayers on the MgO(001) surface. *Phys. Chem. Chem. Phys.* **2018**, *20*, 9760–9769.
- (14) Eichler, U.; Kölmel, C.; Sauer, J. Combining Ab initio Techniques with Analytical Potential Functions for Structure Predictions of Large Systems: Method and Application to Crystalline Silica Polymorphs. *J. Comput. Chem.* **1997**, *18*, 463–477.
- (15) Sierka, M.; Sauer, J. Finding Transition Structures in Extended Systems: A Strategy Based on a Combined Quantum Mechanics – Empirical Valence Bond Approach. *J. Chem. Phys.* **2000**, *112*, 6983–6996.
- (16) Sauer, J.; Sierka, M. Combining Quantum Mechanics and Intermolecular Potential Functions in Ab Initio Studies of Extended Systems. *J. Comput. Chem.* **2000**, *21*, 1470–1493.
- (17) Pople, J. A. Quantum chemical models (Nobel lecture). *Angew. Chem., Int. Ed.* **1999**, *38*, 1894–1902.
- (18) Svelle, S.; Tuma, C.; Rozanska, X.; Kerber, T.; Sauer, J. Quantum Chemical Modeling of Zeolite-Catalyzed Methylation Reactions: Toward Chemical Accuracy for Barriers. *J. Am. Chem. Soc.* **2009**, *131*, 816–825.
- (19) Chung, L. W.; Sameera, W. M. C.; Ramozzi, R.; Page, A. J.; Hatanaka, M.; Petrova, G. P.; Harris, T. V.; Li, X.; Ke, Z.; Liu, F.; Li, H.-B.; Ding, L.; Morokuma, K. The ONIOM Method and Its Applications. *Chem. Rev.* **2015**, *115*, 5678–5796.
- (20) Piccini, G.; Alessio, M.; Sauer, J. Ab Initio Calculation of Rate Constants for Molecule–Surface Reactions with Chemical Accuracy. *Angew. Chem., Int. Ed.* **2016**, *55*, 5235–5237.
- (21) Wesolowski, T. A.; Warshel, A. Frozen density functional approach for ab initio calculations of solvated molecules. *J. Phys. Chem.* **1993**, *97*, 8050–8053.

- (22) Manby, F. R.; Stella, M.; Goodpaster, J. D.; Miller, T. F. A Simple, Exact Density-Functional-Theory Embedding Scheme. *J. Chem. Theory Comput.* **2012**, *8*, 2564–2568.
- (23) Libisch, F.; Huang, C.; Carter, E. A. Embedded Correlated Wavefunction Schemes: Theory and Applications. *Acc. Chem. Res.* **2014**, *47*, 2768–2775.
- (24) Bennie, S. J.; van der Kamp, M. W.; Penniford, R. C. R.; Stella, M.; Manby, F. R.; Mulholland, A. J. A Projector-Embedding Approach for Multiscale Coupled-Cluster Calculations Applied to Citrate Synthase. *J. Chem. Theory Comput.* **2016**, *12*, 2689–2697.
- (25) Ugliengo, P.; Damin, A. Are dispersive forces relevant for CO adsorption on the MgO(001) surface? *Chem. Phys. Lett.* **2002**, *366*, 683–690.
- (26) Kubas, A.; Berger, D.; Oberhofer, H.; Maganas, D.; Reuter, K.; Neese, F. Surface Adsorption Energetics Studied with “Gold Standard” Wave-Function-Based Ab Initio Methods: Small-Molecule Binding to TiO₂(110). *J. Phys. Chem. Lett.* **2016**, *7*, 4207–4212.
- (27) Halkier, A.; Helgaker, T.; Jørgensen, P.; Klopper, W.; Olsen, J. Basis-set convergence of the energy in molecular Hartree–Fock calculations. *Chem. Phys. Lett.* **1999**, *302*, 437–446.
- (28) Jensen, F. Estimating the Hartree–Fock Limit from Finite Basis Set Calculations. *Theor. Chem. Acc.* **2005**, *113*, 267–273.
- (29) Helgaker, T.; Klopper, W.; Koch, H.; Noga, J. Basis-set Convergence of Correlated Calculations on Water. *J. Chem. Phys.* **1997**, *106*, 9639–1997.
- (30) Boys, S. F.; Bernardi, F. B. The Calculation of Small Molecular Interactions by the Differences of Separate Total Energies. Some Procedures with Reduced Errors. *Mol. Phys.* **1970**, *19*, 553–566.
- (31) Sauer, J. Molecular Models in ab initio Studies of Solids and Surfaces: From Ionic Crystals and Semiconductors to Catalysts. *Chem. Rev.* **1989**, *89*, 199–255.
- (32) Kerber, T.; Sierka, M.; Sauer, J. Application of Semiempirical Long-Range Dispersion Corrections to Periodic Systems in Density Functional Theory. *J. Comput. Chem.* **2008**, *29*, 2088–2097.
- (33) Tuma, C.; Kerber, T.; Sauer, J. The tert-Butyl Cation in H-Zeolites: Deprotonation to Isobutene and Conversion into Surface Alkoxides. *Angew. Chem., Int. Ed.* **2010**, *49*, 4678–4680.
- (34) Grimme, S. Semiempirical GGA-type Density Functional Constructed with a Long-Range Dispersion Correction. *J. Comput. Chem.* **2006**, *27*, 1787–1799.
- (35) Rybicki, M.; Sauer, J. Ab Initio Prediction of Proton Exchange Barriers for Alkanes at Bronsted Sites of Zeolite H-MFI. *J. Am. Chem. Soc.* **2018**, *140*, 18151–18161.
- (36) Solans-Monfort, X.; Branchadell, V.; Sodupe, M.; Sierka, M.; Sauer, J. Electron Hole Formation in Acidic Zeolite Catalysts: H-ZSM-5. *J. Chem. Phys.* **2004**, *121*, 6034–6041.
- (37) Alessio, M.; Usvyat, D.; Sauer, J. Chemically Accurate Adsorption Energies: CO and H₂O on the MgO(001) Surface. *J. Chem. Theory Comput.* **2019**, *15*, 1329–1344.
- (38) Sillar, K.; Hofmann, A.; Sauer, J. Ab Initio Study of Hydrogen Adsorption in MOF-5. *J. Am. Chem. Soc.* **2009**, *131*, 4143–4150.
- (39) Kundu, A.; Piccini, G.; Sillar, K.; Sauer, J. Ab initio prediction of adsorption isotherms for small molecules in metal-organic frameworks. *J. Am. Chem. Soc.* **2016**, *138*, 14047–14056.
- (40) Sillar, K.; Kundu, A.; Sauer, J. Ab Initio Adsorption Isotherms for Molecules with Lateral Interactions: CO₂ in Metal–Organic Frameworks. *J. Phys. Chem. C* **2017**, *121*, 12789–12799.
- (41) Piccini, G.; Alessio, M.; Sauer, J.; Zhi, Y.; Liu, Y.; Kolvenbach, R.; Jentys, A.; Lercher, J. A. Accurate Adsorption Thermodynamics of Small Alkanes in Zeolites. Ab initio Theory and Experiment for H-Chabazite. *J. Phys. Chem. C* **2015**, *119*, 6128–6137.
- (42) Zheng, J. J.; Zhao, Y.; Truhlar, D. G. The DBH24/08 Database and Its Use to Assess Electronic Structure Model Chemistries for Chemical Reaction Barrier Heights. *J. Chem. Theory Comput.* **2009**, *5*, 808–821.
- (43) Sylvetsky, N.; Peterson, K. A.; Karton, A.; Martin, J. M. L. Toward a W4-F12 approach: Can explicitly correlated and orbital-based ab initio CCSD(T) limits be reconciled? *J. Chem. Phys.* **2016**, *144*, 214101.
- (44) Dohnálek, Z.; Kimmel, G. A.; Joyce, S. A.; Ayotte, P.; Smith, R. S.; Kay, B. D. Physisorption of CO on the MgO(100) Surface. *J. Phys. Chem. B* **2001**, *105*, 3747–3751.
- (45) Tait, S. L.; Dohnalek, Z.; Campbell, C. T.; Kay, B. D. n-alkanes on MgO(100). Coverage dependent desorption kinetics of n-butane. *J. Chem. Phys.* **2005**, *122*, 164707.
- (46) Mulder, F. M.; Dingemans, T. J.; Schimmel, H. G.; Ramirez-Cuesta, A. J.; Kearley, G. J. Hydrogen adsorption strength and sites in the metal organic framework MOF5: Comparing experiment and model calculations. *Chem. Phys.* **2008**, *351*, 72–76.
- (47) Dinca, M.; Han, W. S.; Liu, Y.; Dailly, A.; Brown, C. M.; Long, J. R. Observation of Cu²⁺–H₂ Interactions in a Fully Desolvated Sodalite-Type Metal–Organic Framework. *Angew. Chem., Int. Ed.* **2007**, *46*, 1419–1422.
- (48) Bloch, E. D.; Hudson, M. R.; Mason, J. A.; Chavan, S.; Crocellà, V.; Howe, J. D.; Lee, K.; Dzubak, A. L.; Queen, W. L.; Zadrozny, J. M.; Geier, S. J.; Lin, L.-C.; Gagliardi, L.; Smit, B.; Neaton, J. B.; Bordiga, S.; Brown, C. M.; Long, J. R. Reversible CO Binding Enables Tunable CO/H₂ and CO/N₂ Separations in Metal–Organic Frameworks with Exposed Divalent Metal Cations. *J. Am. Chem. Soc.* **2014**, *136*, 10752–10761.
- (49) Queen, W. L.; Hudson, M. R.; Bloch, E. D.; Mason, J. A.; Gonzalez, M. I.; Lee, J. S.; Gygi, D.; Howe, J. D.; Lee, K.; Darwish, T. A.; James, M.; Peterson, V. K.; Teat, S. J.; Smit, B.; Neaton, J. B.; Long, J. R.; Brown, C. M. Comprehensive study of carbon dioxide adsorption in the metal-organic frameworks M2(dobdc) (M = Mg, Mn, Fe, Co, Ni, Cu, Zn). *Chem. Sci.* **2014**, *5*, 4569–4581.
- (50) Svelle, S.; Ronning, P. A.; Kolboe, S. Kinetic studies of zeolite-catalyzed methylation reactions 1. Coreaction of [C-12]ethene and [C-13]methanol. *J. Catal.* **2004**, *224*, 115–123.
- (51) Svelle, S.; Ronning, P. O.; Olsbye, U.; Kolboe, S. Kinetic studies of zeolite-catalyzed methylation reactions. Part 2. Co-reaction of [C-12]propene or [C-12]n-butene and [C-13]methanol. *J. Catal.* **2005**, *234*, 385–400.
- (52) Hansen, N.; Kerber, T.; Sauer, J.; Bell, A. T.; Keil, F. J. Quantum Chemical Modeling of Benzene Ethylation over H-ZSM-5 Approaching Chemical Accuracy: A Hybrid MP2:DFT Study. *J. Am. Chem. Soc.* **2010**, *132*, 11525–11538.
- (53) Kolos, W. Hydrogen molecule. Test of quantum chemistry. *Polym. J. Chem.* **1993**, *67*, 553–566.
- (54) Pacchioni, G. Quantum chemistry of oxide surfaces: From CO chemisorption to the identification of the structure and nature of point defects on MgO. *Surf. Rev. Lett.* **2000**, *7*, 277–306.
- (55) Nygren, M. A.; Pettersson, L. G. M. Comparing ab initio computed energetics with thermal experiments in surface science: CO/MgO(001). *J. Chem. Phys.* **1996**, *105*, 9339–9348.
- (56) Wichtendahl, R.; Rodriguez-Rodrigo, M.; Härtel, U.; Kühlenbeck, H.; Freund, H. J. TDS study of the bonding of CO and NO to vacuum-cleaved NiO(100). *Surf. Sci.* **1999**, *423*, 90–98.
- (57) Spoto, G.; Gribov, E. N.; Ricchiardi, G.; Damin, A.; Scarano, D.; Bordiga, S.; Lamberti, C.; Zecchina, A. Carbon monoxide MgO from dispersed solids to single crystals: a review and new advances. *Prog. Surf. Sci.* **2004**, *76*, 71–146.
- (58) Spoto, G.; Gribov, E.; Damin, A.; Ricchiardi, G.; Zecchina, A. The IR spectra of Mg²⁺_{sc} (CO) complexes on the (001) surfaces of polycrystalline and single crystal MgO. *Surf. Sci.* **2003**, *540*, L605–L610.
- (59) Furukawa, H.; Cordova, K. E.; O’Keeffe, M.; Yaghi, O. M. The Chemistry and Applications of Metal–Organic Frameworks. *Science* **2013**, *341*, 1230444.
- (60) Park, J.; Howe, J. D.; Sholl, D. S. How Reproducible Are Isotherm Measurements in Metal–Organic Frameworks? *Chem. Mater.* **2017**, *29*, 10487–10495.
- (61) Sillar, K.; Sauer, J. Ab Initio Prediction of Adsorption Isotherms for Small Molecules in Metal–Organic Frameworks: The Effect of Lateral Interactions for Methane/CPO-27-Mg. *J. Am. Chem. Soc.* **2012**, *134*, 18354–18365.
- (62) Dietzel, P. D. C.; Besikiotis, V.; Blom, R. Application of metal–organic frameworks with coordinatively unsaturated metal sites in

storage and separation of methane and carbon dioxide. *J. Mater. Chem.* **2009**, *19*, 7362–7370.

(63) Tuma, C.; Sauer, J. Protonated Isobutene in Zeolites: tert-Butyl Cation or Alkoxide? *Angew. Chem., Int. Ed.* **2005**, *44*, 4769–4771.

(64) Plessow, P. N.; Smith, A.; Tischer, S.; Studt, F. Identification of the Reaction Sequence of the MTO Initiation Mechanism Using Ab Initio-Based Kinetics. *J. Am. Chem. Soc.* **2019**, *141*, 5908–5915.

(65) Piccini, G.; Alessio, M.; Sauer, J. Ab initio study of methanol and ethanol adsorption on Brønsted sites in zeolite H-MFI. *Phys. Chem. Chem. Phys.* **2018**, *20*, 19964–19970.

(66) Tuma, C.; Sauer, J. Quantum chemical ab initio prediction of proton exchange barriers between CH₄ and different H-zeolites. *J. Chem. Phys.* **2015**, *143*, 102810.

(67) Truitt, M. J.; Toporek, S. S.; Rovira-Truitt, R.; White, J. L. Alkane C-H bond activation in zeolites: Evidence for direct protium exchange. *J. Am. Chem. Soc.* **2006**, *128*, 1847–1852.

(68) Sommer, J.; Habermacher, D.; Jost, R.; Sassi, A.; Stepanov, A. G.; Luzgin, M. V.; Freude, D.; Ernst, H.; Martens, J. Activation of Small Alkanes on Solid Acids. An H/D Exchange Study by Liquid and Solid-State NMR: The Activation Energy and the Inhibiting Effect of Carbon Monoxide. *J. Catal.* **1999**, *181*, 265–270.

(69) Schoofs, B.; Schuermans, J.; Schoonheydt, R. A. Hydrogen-deuterium exchange reactions with isobutane over acid zeolites. *Microporous Mesoporous Mater.* **2000**, *35–36*, 99–111.

(70) Xue, N.; Vjunov, A.; Schallmoser, S.; Fulton, J. L.; Sanchez-Sanchez, M.; Hu, J. Z.; Mei, D.; Lercher, J. A. Hydrolysis of zeolite framework aluminum and its impact on acid catalyzed alkane reactions. *J. Catal.* **2018**, *365*, 359–366.

(71) Wu, T.; Werner, H.-J.; Manthe, U. First-principles theory for the H+CH₄ → H₂ + CH₃ Reaction. *Science* **2004**, *306*, 2227–2229.

(72) Catlow, C. R. A. Prediction of Rate Constants for Catalytic Reactions with Chemical Accuracy. *Angew. Chem., Int. Ed.* **2016**, *55*, 9132–9133.

(73) Chen, G. P.; Voora, V. K.; Agee, M. M.; Balasubramani, S. G.; Furche, F. Random-Phase Approximation Methods. *Annu. Rev. Phys. Chem.* **2017**, *68*, 421–445.

(74) Göttl, F.; Gruneis, A.; Bucko, T.; Hafner, J. Van der Waals Interactions between Hydrocarbon Molecules and Zeolites: Periodic Calculations at Different Levels of Theory, from Density Functional Theory to the Random Phase Approximation and Moeller-Plesset Perturbation Theory. *J. Chem. Phys.* **2012**, *137*, 114111.